Oil & Gas Science and Technology – Rev. IFP Energies nouvelles, Vol. 66 (2011), No. 1, pp. 47-65

DOI: 10.2516/ogst/2010016

IFP Energies nouvelles International Conference
Rencontres Scientifiques d'IFP Energies nouvelles

Deep Saline Aquifers for Geological Storage of CO_2 and Energy
Stockage géologique du CO_2 et de l'énergie en aquifères salins profonds

Reservoir Characterization for CO_2 Sequestration: Assessing the Potential of the Devonian Carbonate Nisku Formation of Central Alberta

C. Eisinger[1*] and J. Jensen[2]

1 University of Calgary, Energy and Environmental Systems Group, 2500 University Drive NW, Calgary, AB T2N 1N4 - Canada
2 University of Calgary, Department of Chemical and Petroleum Engineering, 2500 University Drive NW, Calgary, AB T2N 1N4 - Canada
e-mail: chris.eisinger@ucalgary.ca - jjensen@ucalgary.ca

* Current Address: Colorado Geological Survey, 1313 Sherman Street, Rm. 715, Denver, CO, 80203 - USA
e-mail: chris.eisinger@state.co.us

Résumé – Caractérisation de réservoir en vue du stockage géologique de CO_2 : évaluation du potentiel offert par les carbonates dévoniens de la formation de Nisku, en Alberta central – Plusieurs gros émetteurs de CO_2, totalisant 30 Mt annuels, sont localisés dans la région du Lac Wabamun, au centre de l'Alberta (Canada). Des études antérieures ont montré le potentiel offert par les aquifères salins profonds de la région pour le stockage géologique de ce gaz et le présent article rend compte d'une caractérisation des carbonates dévoniens de la formation Nisku, en vue de réaliser un stockage de CO_2.

Une telle caractérisation doit surmonter plusieurs handicaps : données de puits et de sismique réflexion assez rares et dispersées, tests en forage de qualité médiocre et rareté des mesures modernes. Des diagraphies de porosité ne sont disponibles que pour un tiers des puits, de sorte qu'on a utilisé les diagraphies de résistivité pour évaluer la porosité et la transmissivité (perméabilité × épaisseur). Le facteur de cimentation d'Archie vaut entre 2 et 3, ce qui maintient une incertitude quant à l'estimation de la porosité ainsi obtenue ; toutefois, on peut identifier les intervalles de forte porosité. En ce qui concerne la transmissivité, les valeurs déduites des logs sont mieux corrélées à celles provenant des mesures sur carotte qu'à celles obtenues par DST ou test de production. Un tel comportement n'est pas surprenant, car les tests sont moins sensibles à l'occurrence très locale de bancs rendus extrêmement perméables par une porosité vacuolaire (*vuggy* ou *moldic*).

La distribution des faciès sédimentaires a été modélisée à l'aide de deux approches, de type "pixel" ou de type "objet". La seconde, qui utilise des dimensions obtenues par imagerie satellitaire sur des environnements actuels, fournit des résultats plus cohérents avec la compréhension géologique que l'on a de la formation de Nisku, et se traduit par une connectivité à large échelle supérieure à celle obtenue par la méthode "pixel". Les volumes obtenus indiquent une capacité potentielle de stockage considérable dans cette formation, toutefois les simulations hydrauliques laissent penser que l'injectivité initiale resterait inférieure à 20 Mt/an (objectif souhaité), pour les puits verticaux. Un *design* plus élaboré des puits d'injection, avec la prise en compte de stimulation par fracturation et/ou de puits latéraux multiples, pourrait permettre d'atteindre l'objectif d'injection indiqué.

Abstract — Reservoir Characterization for CO_2 Sequestration: Assessing the Potential of the Devonian Carbonate Nisku Formation of Central Alberta *— The Wabamun Lake area of Central Alberta, Canada includes several large CO_2 point source emitters, collectively producing more than 30 Mt annually. Previous studies established that deep saline aquifers beneath the Wabamun Lake area have good potential for the large-scale injection and storage of CO_2. This study reports on the characterization of the Devonian carbonate Nisku Formation for evaluation as a CO_2 repository.*

Major challenges for characterization included sparse well and seismic data, poor quality flow tests, and few modern measurements. Wireline porosity measurements were present in only one-third of the wells, so porosity and flow capacity (permeability-thickness) were estimated using wireline electrical measurements. The Archie cementation factor appears to vary between 2 and 3, creating uncertainty when predicting porosity using the electrical measurements; however, high-porosity zones could be identified. The electrically-based flow capacity predictions showed more favorable values using a correlation with core than the relation based on drill stem and production tests. This behavior is expected, since the flow test flow capacities are less influenced by local occurrences of very permeable vuggy and moldic rocks.

Facies distributions were modeled using both pixel and object methods. The object models, using dimensions obtained from satellite imaging of modern day environments, gave results that were more consistent with the geological understanding of the Nisku and showed greater large-scale connectivity than the pixel model. Predicted volumes show considerable storage capacity in the Nisku, but flow simulations suggest injection capacities are below an initial 20 Mt/year target using vertical wells. More elaborate well designs, including fracture stimulation or multi-lateral wells may allow this goal to be reached or surpassed.

INTRODUCTION

The Wabamun Lake area of Central Alberta, Canada includes several large CO_2 point source emitters, with combined annual production exceeding 30 Mt (Environment Canada, 2009). The largest sources are four coal-fired power plants with more than 4000 MW total generating capacity between them *(Fig. 1)*. Geological sequestration of these emissions will play a role in helping Alberta reduce its > 230 Mt total output of greenhouse gases (GHG) (Environment Canada, 2009), and allow Canada to decrease its overall atmospheric contributions significantly.

Deep saline aquifers provide an attractive target for GHG injection and sequestration for a number of reasons, including:
- the high potential storage capacity (> 4000 Gt CO_2) and accessibility on a regional scale;
- a minimal likelihood for interference with existing hydrocarbon producing fields and plays;
- the limited or non-existent utility of saline water;
- an aquifer abundance at a variety of stratigraphic intervals and lithologies allowing for flexibility in drilling and storage.

Characterization of these reservoirs is critical, especially understanding the lithologies, trapping and sealing mechanisms, and the regional geomechanics. Geomechanics and brine geochemistry also have important roles in understanding potential injection and storage.

In selecting aquifers most suitable for CO_2 injection, some key criteria are:
- aquifer depth; the aquifer needs to be sufficiently deep to allow pressures and temperatures necessary for CO_2 to exist as a super critical fluid (*i.e.* 31.1 C and 7.8 MPa) but not so deep as to have little permeability (reservoir quality);
- proximal barriers; there should exist multiple impermeable and low-permeability horizons (*i.e.* aquitards and aquicludes) between the target aquifer and the surface to minimize leakage risk;
- interference with existing activities; there should be no impact on existing hydrocarbon production.

Using these simple criteria, the best aquifer targets in the Wabamun Lake area are the Paleozoic passive-margin carbonates and basal Cambrian sandstones. A saline aquifer, the Devonian Nisku *(Fig. 2)*, is of particular interest as its depth, thickness, and stratigraphic configuration appear to be well suited for CO_2 injection and storage.

The goal of this study was to generate cell-based, heterogeneous static geological models using all available data. Modeling was geared towards producing suitable inputs for flow simulations of CO_2 injection and storage over 100 years. The methods for data integration, analysis, and workflow in reservoir characterization of CO_2 sequestration are key aspects. The study emphasis is as much on the process steps as the results.

1 PREVIOUS WORK

Previous studies established that deep saline aquifers beneath the Wabamun Lake area have good potential for the large-scale injection and storage of CO_2 (Michael *et al.*, 2009; Hitchon, 1996). Geological characterization and modeling results from the study by Michael and co-workers laid the foundation for our work. Their comprehensive characterization identified the Nisku as a prime aquifer target, assessing the sedimentary succession, hydrogeological conditions, rock characteristics, and *in-situ* fluid properties. Preliminary fluid flow models for homogeneous conditions predict the Nisku injection capacity to be > 10 Mt/year for 30 years (Michael *et al.*, 2009). Results from heterogeneous models in this study suggest a much lower potential capacity.

The geological setting for subsurface Paleozoic sediments in the Wabamun region is described extensively in the Western Canada Sedimentary Basin Atlas (Ch. 7-15, Mossop and Shetson, 1994). Descriptions of geology and sedimentary succession for the Upper Devonian Nisku Formation are provided by Watts (1987), Stoakes (1987, 1992), Switzer *et al*. (1994), and Michael *et al*. (2009). Available pre-existing mineralogical and geochemical data are limited (Simpson, 1999; Michael *et al*., 2009), and thus samples were collected and analyzed for this project.

2 WABAMUN AREA SEQUESTRATION PROJECT

The Wabamun Area Sequestration Project (WASP) is a feasibility study centered on a region southwest of Edmonton,

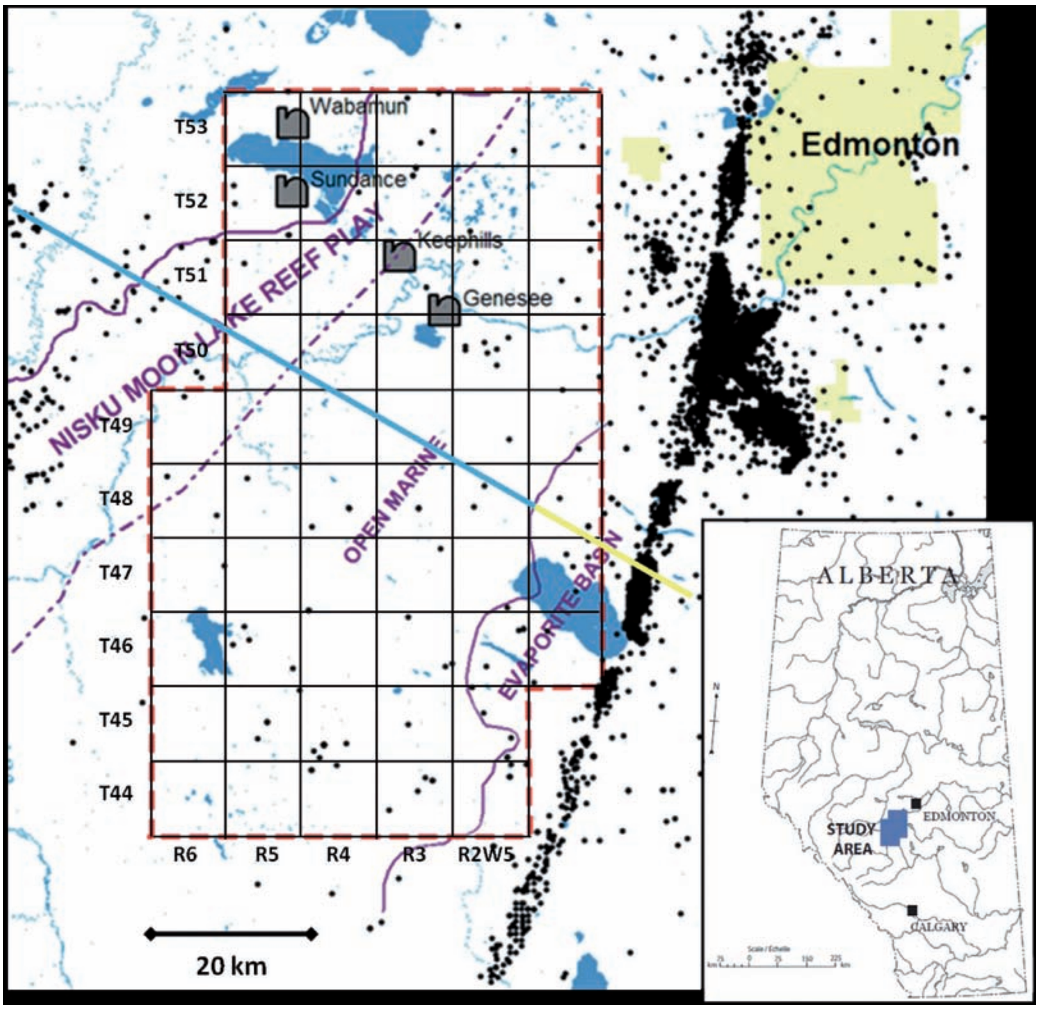

Figure 1

The WASP study area (red outline) and locations of four large coal-fired power plants. Black circles show wells that penetrate the Nisku Formation. Purple lines mark important depositional boundaries of the Upper Devonian. The study area has an areal extent of approximately 5000 km^2.

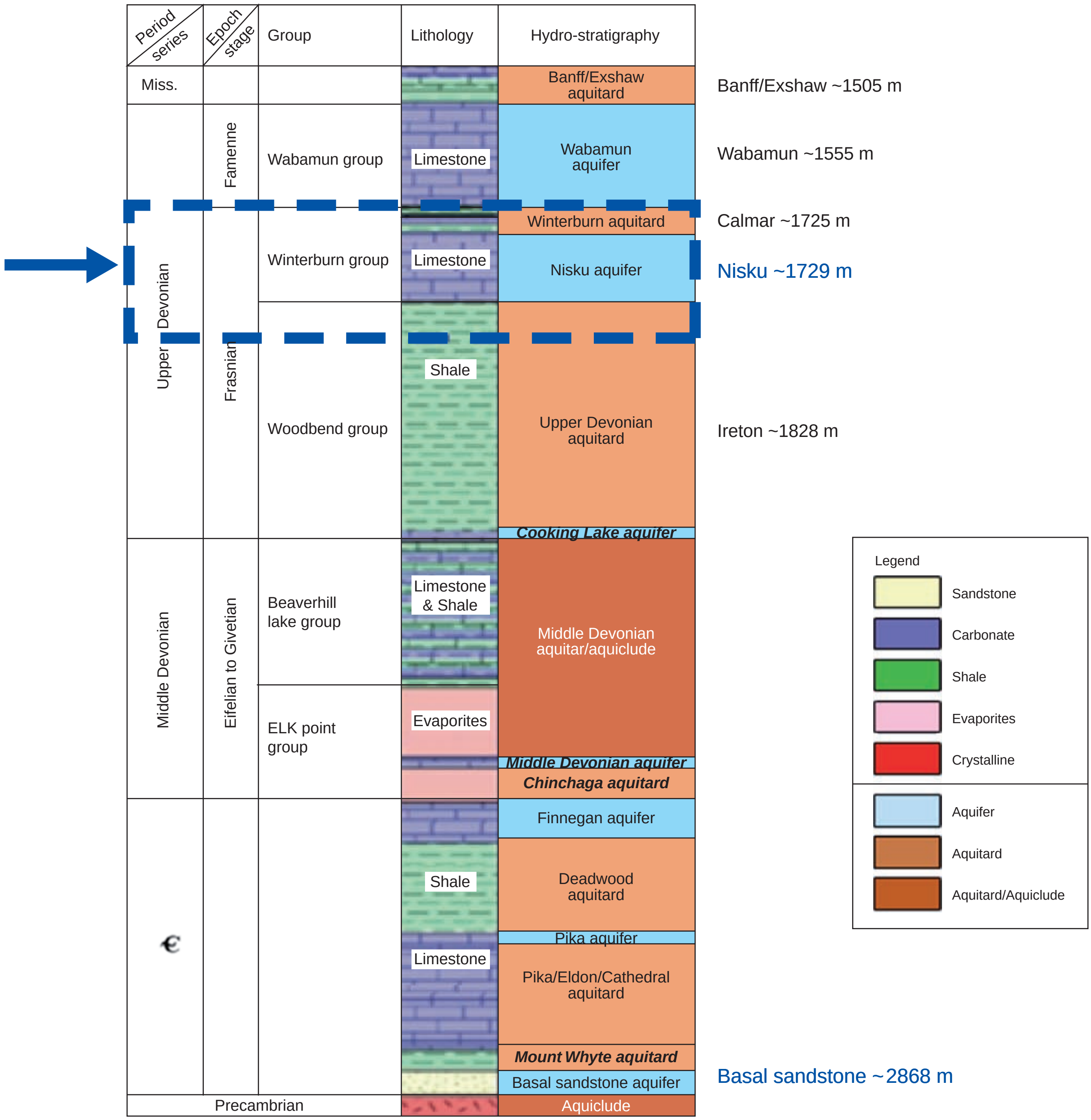

Figure 2

Paleozoic stratigraphy for WASP region (modified after *Fig. 2* in Bachu and Bennion, 2008). Depth, absence of hydrocarbons, and aquifer-aquitard configuration supports Upper Devonian Nisku Fm. as prime CO_2 injection candidate. Another possible storage aquifer is the basal Cambrian sandstone.

Alberta *(Fig. 1)* with a total areal extent in excess of 5130 km^2. The Area of Interest (AOI) encompasses 60 townships (57.96 km × 96.6 km) of predominantly agricultural and recreational land use. This broad area of investigation provides several saline aquifer targets in the subsurface, stratigraphic configurations optimal for storage and trapping of CO_2, and sufficient areal extent for placing wells at optimal injection spacings. Additionally, the distance to CO_2 point source emitters is reasonable for pipeline and other surface infrastructure considerations.

The WASP project targeted the sub-Cretaceous aquifers in the region *(Fig. 2)* to allow for depths below 900 m that would provide suitable pressure and temperature conditions for CO_2 injection and storage. Potential injection targets originally included a basal Cambrian sand, 30 m thick on average; several thin carbonate aquifers (< 25 m) in the Cambrian and Middle Devonian; and the Nisku and Wabamun aquifers (both > 60 m thick) in the Upper Devonian. As recognized in previous studies (*e.g.*, Michael *et al.*, 2009), data and drilling considerations limit possible targets to the Upper Devonian (*i.e.* the Nisku and Wabamun Formations) at the present. Of the two sequestration candidates, the Nisku Fm. is more suitable due to its having the extra Winterburn aquitard above it, and less likelihood of interference with current or future hydrocarbon production in the area.

3 GEOLOGICAL SETTING

The Paleozoic sedimentary sequence for the WASP study area begins with passive margin sandstones of Cambrian age, before a long depositional period of marine carbonates, shales, and occasional evaporites throughout the Devonian and Mississippian *(Fig. 2)*. The overlying Cretaceous formations are predominantly siliciclastics – sandstones, siltstones, and shales. The combined Cretaceous and pre-Cretaceous section is greater than 2000 m thick in the study area, with the depth to the top of the Nisku Formation between 1000 m in the NE and 2000 m in the SW. The entire sedimentary package dips gently from NE to SW approximately 0.5 degrees on average through the study area. Being part of the Western Canadian Sedimentary Basin (WCSB), the stratigraphic continuity of the targeted layers extends to the east and northeast by > 200 km (Mossop and Shetson, 1994).

Structurally, the area of interest is regionally stable with minimal faulting (Frank Stoakes, personal communication, 2009). From both regional and focused seismic data analysis, displacements within the Nisku or surrounding strata were absent (Alsuhail *et al.*, 2009). Integrity of the caprock (the Calmar Fm.) appears to be very good with few points of potential upward flow. A source of concern is possible karsting in an overlying carbonate formation (the Wabamun Fm.) that may weaken the compentency of layers directly above the Nisku. Small, isolated features (< 1 km in diameter) interpreted from seismic data may influence the choices for injection well locations.

Nisku deposition occurs as the earliest part of the Winterburn Group, subsequent to shales and carbonates nearly filling the WCSB. The Nisku interval represents a strong marine transgression with carbonate ramp deposition dominant (Switzer *et al.*, 1994). Indications suggest a late stage regressive episode as well, but deposition diminished during this time in the area of interest (Switzer *et al.*, 1994).

For the WASP region, the Nisku interval includes open marine ramp carbonates, shallower platform carbonates, and peritidal hypersaline facies *(Fig. 3)*. Thickness of the Nisku carbonate accumulation ranges from 40 m near the eastern boundary of the study area to over 100 m closer to the shelf margin. Basinward are hydrocarbon bearing pinnacle reefs (Zeta Pinnacle Trend) and shelf margin reefs (Moon Lake Build-Ups). These mark the western boundary of the potential injection aquifer. The transition from open marine carbonate facies to the low permeability hypersaline rocks of a paleo-evaporite basin delineates the eastern boundary *(Fig. 3)*.

For the WASP study, two facies assemblages were identified from the limited core available: an undifferentiated

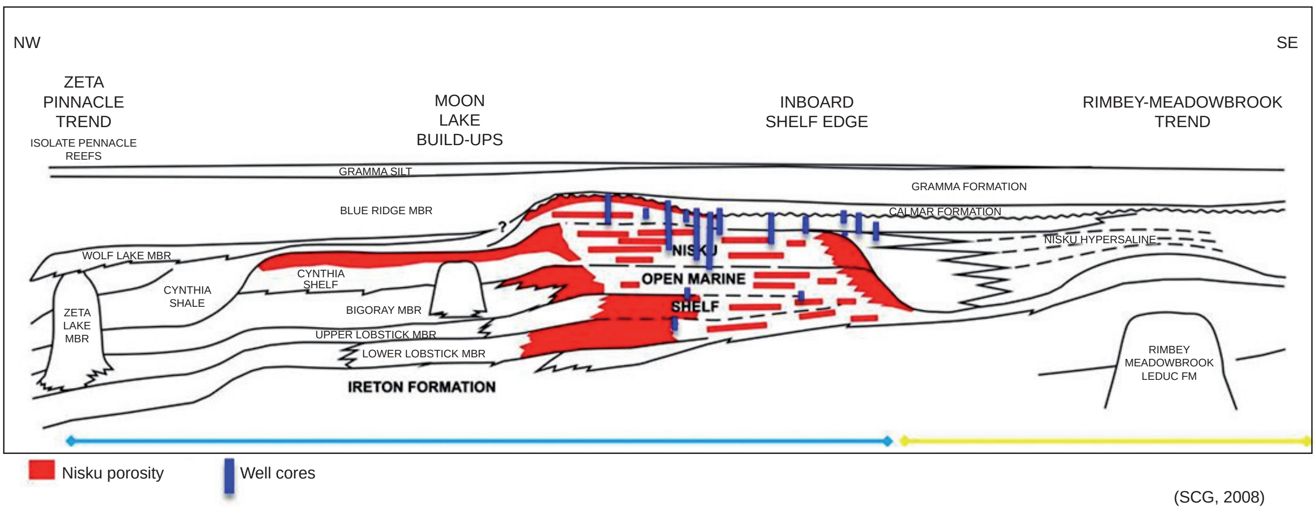

Figure 3

A conceptual NE-SW cross-section (see blue-yellow line in *Fig. 1*) through the Nisku formation for WASP (used with permission from SCG Ltd). Red shading indicates regions of enhanced porosity and vertical blue columns represent stratigraphic position of well cores. Most cores sample the upper portion of the Nisku, where porosity is typically poorer than the lower parts.

a)

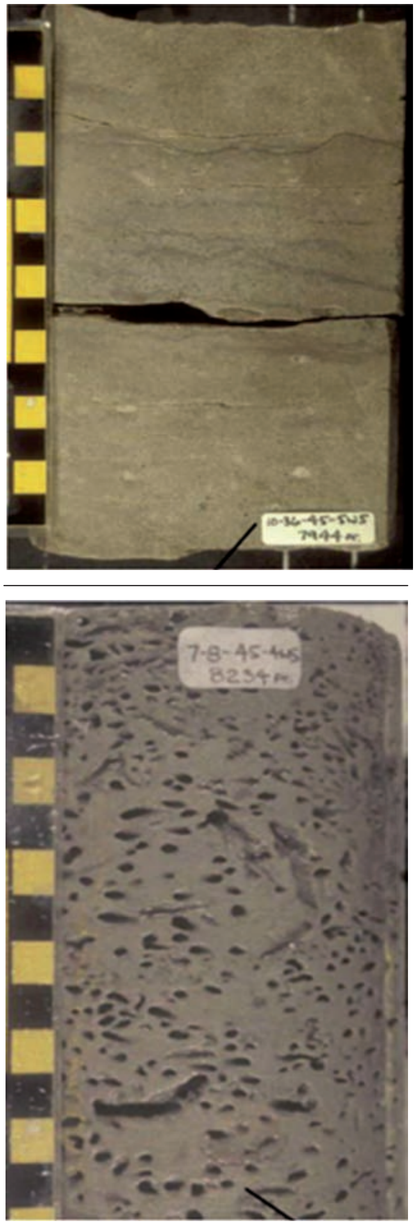

b)

Figure 4

a) Hypersaline facies core sample: dolomitic mudstone to grainstone with anhydrite plugging; porosity = 1.7% and k_{max} = 3 mD.

b) Open marine facies core samples: upper photo – common dolomitic mudstone to grainstone; porosity = 3-5% and k_{max} = 5-15 mD. Lower photo – rare dolimitic grainstone to boundstone with Amphipora derived vugs; porosity = 14% and k_{max} > 10 000 mD.

open marine facies (including shallower platform carbonates) and a hypersaline carbonate mudstone. The hypersaline facies *(Fig. 4a)* consists of dolomitic mudstone to grainstone with occasional moldic porosity and limited Amphipora. Abundant anhydrite and fine-grained silt and shale stringers reduce the permeability significantly. Core permeabilities are less than 5 mD (5×10^{-3} μm^2) and porosity is typically less than 2%. The open marine facies *(Fig. 4b)* includes dolomitic mudstone to boundstone. Vuggy and moldic porosity are observed in some intervals, while anhydrite plugging is limited. Stromatoporoids and Amphipora are common, with less frequent corals and brachiopods also present. Core porosities are typically between 3 to 5%, and permeabilities between 5 to 15 mD. In exceptional cases, porosity exceeds 12%, with permeabilities of several Darcys.

The Nisku shelf is underlain by Ireton Fm. shales and overlain by fine-grained clastics of the Calmar Fm. – a persistent, low-permeability shale unit typically between

5 and 12 m thick. Above, the Calmar Fm. is the Graminia Fm. (including the Blue Ridge Member), which collectively comprise the Winterburn aquitard *(Fig. 2)*.

4 CHARACTERIZATION OF THE NISKU FORMATION

4.1 Data

With an area of more than 5000 km^2 for the WASP AOI, Nisku formation data are clearly sparse. As is likely to be the case for other deep saline aquifers, Nisku characterization is hampered by infrequent penetrating wells, limited core, and often patchy wireline log coverage. For building static and dynamic models, the available information includes:

– data from 96 wells that penetrate the Nisku within the AOI, including paper tour (drilling) reports;
– wireline geophysical logs of varying vintage, from the 1950's to recent suites;
– routine core analyses and lithological descriptions for 13 wells in the study area, with special core analyses for select samples;
– processed and raw geophysical data;
– Drill Stem Tests (DSTs) of generally poor quality;
– petrographic studies, both publicly available and newly acquired.

The distribution of data presents a challenge for accurate modeling in the inter-well zones *(Fig. 5)*. Inter-well distances range from 0.5 km to more than 20 km.

For each well, information is available for the location and depth, the historical status of operation (*e.g.*, drilling rig tour sheets), and in some cases, well casing and completion. Production data are scarce for the Nisku interval as very few wells have produced. One notable exception is a water-production well (1F1/11-29-045-02W5/00) that has recorded data since January, 2003. Core from thirteen wells was also logged. Cores are 2.5 cm, 7.5 cm, or 10 cm diameter, represent a small portion of the Nisku interval (usually < 20 m), and sample only the uppermost section. Prior to this study, six wells with core already had routine (either whole-core or core plug) core analysis performed. For this project, cores from eight additional wells were sent for routine analyses. Core plugs provided measurements of porosity, permeability, and in most cases grain density. Two of these wells were outside the study area *(Fig. 5)*. Special core analyses (directional permeability and compressibility measurements) were obtained for a subset of collected cores.

Wireline geophysical logs exist for 93 of the 96 wells in the study area. Log type and quality largely depend on the vintage *(Tab. 1)*. Of these 93 wells, digitized logs for 79 wells were used in the analysis and interpretation. An additional two wells that penetrate the Nisku Formation outside the study area were included for modeling as they provided core data in lower Nisku intervals. Digital log depth sampling intervals varied between 0.1 m, 0.15 m, 0.2 m, 0.5 m, and 0.6 m. All digitized logs were re-sampled at 0.5 m or 0.6 m. A critical step before petrophysical analysis is quality control of the digitized data, involving checks for unit consistency and accuracy, depth shifting (where possible), and general comparisons with the raster logs for errors in scaling and/or digitization. Stratigraphic picks were primarily based on geophysical logs with Nisku facies distinctions influenced by core observations and facies isopach mapping. Formation tops were individually verified to assure consistency in mapped surfaces.

TABLE 1

Well log availability for the WASP AOI

No. of wells	Age of logs	Log types
35	Pre-1960	SP, resistivity
34	1960-1980	resistivity, porosity
24	Post-1980	full suite

Seismic data were obtained from pre-existing surveys made to evaluate shallower horizons. The available data consist of 199 2D lines, and seven 3D volumes acquired between 1980 and 2003. Data processing and interpretation was focused on a subset region *(Fig. 5)*, selected on the basis of available seismic data, proximity to potential point source emitters, and a general understanding of the area geology. Seismic 3D volumes processed for time structure and impedance of the Nisku Fm. were incorporated into the geomodeling process, and provided more detailed information where coverage exists.

Horner plot analysis of 22 DSTs was useful for estimating reservoir pressures, the average pressure behavior over time, and providing estimates of flow capacity (*i.e.* the product of permeability and thickness). The DSTs were generally poor in quality and targeted only limited intervals of the Nisku Fm.

4.2 Petrophysics

Core porosities, obtained for 13 wells, ranged from 1% to greater than 20%, and maximum permeabilities, k_{max}, were highly variable, between 0.01 mD and > 10 D. The median k_{max} is approximately 10 mD and anisotropy, as measured by the vertical-to-horizontal ratio, $k_v/k_{max} \geq 0.1$ for 68% and $k_v/k_{max} \geq 0.01$ for 88% of the 285 whole-core samples. Core flow capacity (kh) for 7 wells from the uppermost Nisku suggest potential aquitard qualities; more than 75% of the measurements are below 10 mD-m. The core data are mostly from the less porous, uppermost parts of the open marine facies. Statistically, there is not a significant difference in measured porosities or permeabilities relative to position in the carbonate ramp sequence.

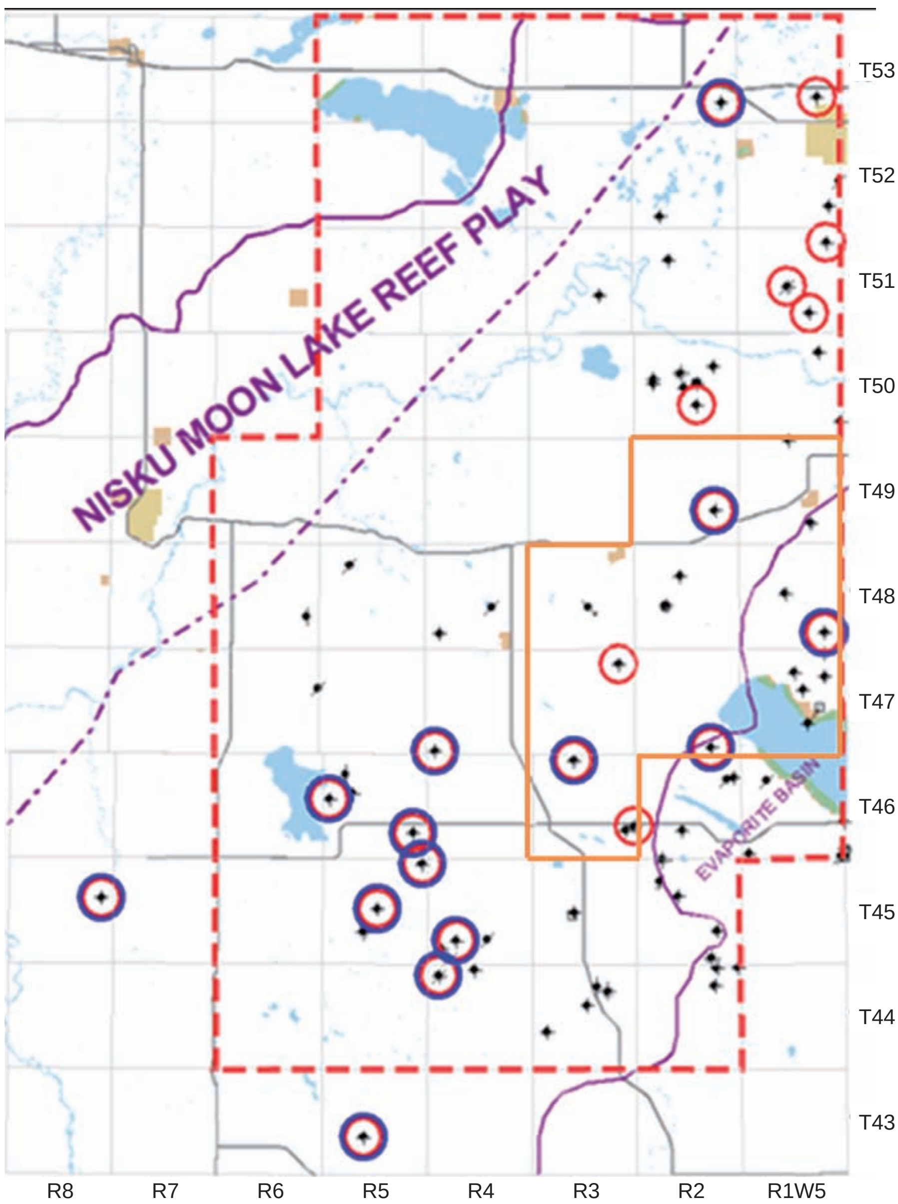

Figure 5

Distribution of available well core data (red circles) for the Nisku Formation. Core analyses (blue circles) from existing (6 wells) and newly acquired (8 wells) data sets. Orange line delineates focus area for seismic data processing and interpretation.

Wireline geophysical well logs for the Nisku aquifer, once properly calibrated to core, quality controlled, and resampled to ensure consistent sampling intervals, provide the basis for much of the static geological modeling. A resolution of 0.3 m or less is desirable for capturing large porosity and permeability occurrences in the open marine Nisku facies. The resolution of many of the older log measurements, however, is poorer than 0.3 m.

Interpretation of porosity measurements in carbonate lithologies is not straight forward, although it is generally assumed that acoustic methods are more sensitive to interparticle porosity, whereas neutron and density logs estimate total porosity (Lucia, 2007). For the WASP AOI, there exist 32 wells with sonic logs available. Porosity was estimated using the relationship of Wyllie *et al*. (1956):

$$\phi_s = (\Delta t - \Delta t_{ma})/(\Delta t_L - \Delta t_{ma}) \quad (1)$$

where ϕ_s = porosity; Δt = tool measured interval transit time; Δt_{ma} = transit time of matrix material; and Δt_L = transit time of interstitial fluid. The assumed values for the Nisku carbonate are Δt_{ma} = 143 μs/m (suitable for a dolomite) and Δt_L = 623 μs/m for the Nisku Fm. fluid. In the cored intervals, the vast majority of samples included mostly interparticle porosity with occasional moldic porous zones. The separate-vug porosity was generally less than a few percent of the total porosity, suggesting that the Wyllie time-average could provide useful estimates (Lucia, 2007). The sonic porosity tends to overestimate core porosity *(Fig. 6)*. This may be caused by anhydrite in the cored intervals, which has a larger transit time (164 μs/m) than that used assuming dolomite in Equation (1). The 13 wells containing coincident density and neutron logs suggest most of the Nisku Fm. samples are dolostone. There are also occasional indications of dolomitic limestone and silty-mudstones in the wireline logs.

There are just over 50 wells that have deep resistivity or conductivity logs, distributed over an extensive portion of the WASP study region. Given the lack of porosity logs in most wells and the water-saturated conditions, we assessed the use of the more abundant resistivity logs to estimate porosity. Archie (1942) proposed that, in 100% water-saturated rocks, porosity depends on rock resistivity (R_o), water resistivity (R_w), and the pore geometry/cementation factor (m):

$$\phi = (R_w/R_o)^{1/m} \tag{2}$$

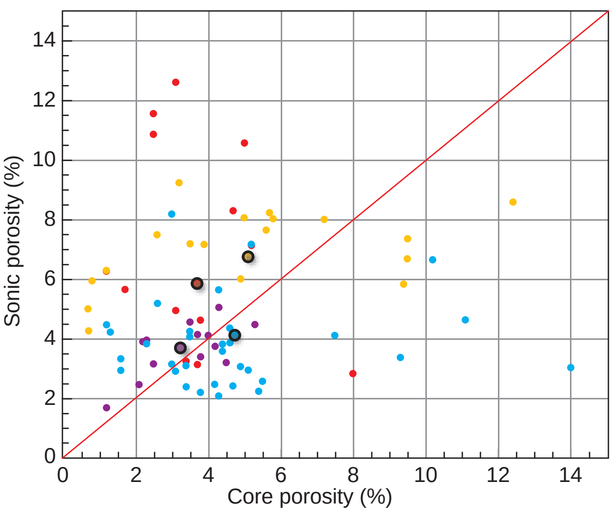

Figure 6

Cross-plot of core porosity estimates *versus* acoustic log estimates for 4 wells (07-08-045-04W5; 07-31-044-04W5; 06-02-047-02W5; 11-24-045-08W5). Larger circles represent average values for each well (shown in different colors) with coincident data available.

R_w = 0.029 ohm-m, based on direct measurement of samples from a water source well in the Nisku and other R_w measurements collected during drilling. R_o was estimated using the deepest resistivity measurement available in the log suite, *e.g.*, deep induction. No environmental corrections were applied to the resistivity log values and R_w is sufficiently small that surface conduction effects could be neglected (Attia *et al*., 2008).

To use Equation (2) requires a value for m. Using wireline measurements from deep induction and density-neutron logs, $2 < m < 3$ *(Fig. 7)*. We observe a similar range for m using core porosities. This range is consistent with values of m obtained in other carbonate formations (Lucia, 2007). The variation in porosity values predicted using Equation (2) arising from the uncertainty in m limits the utility of the resistivity measurements for predicting the actual value of porosity. However, Figure 7 suggests that, if we assume $m = 2$, the resistivity is a useful indicator of minimum porosity, with $R_o < 10$ ohm-m corresponding with $\phi > 5\%$, and $R_o < 5$ ohm-m corresponding with $\phi > 8\%$. Analysis of the resistivity logs assuming $m = 2$ indicates that areas located in the central portion of the Nisku ramp sequence have potentially good porosity, and porosity is larger towards the base of the Nisku Fm. These observations of good porosity, however, may be pessimistic because the poor vertical resolution of the older resistivity logs causes the apparent minimum R_o value for the Nisku interval in a well ($R_{o,min}$) to be overestimated.

Since electrical flow and fluid flow share the same governing equations, we assessed the use of electrical conductivity measurements from wireline to predict hydraulic conductivity. The length of the current path through the formation is directly related to the shape, diameter, and sorting of the grains, geometric packing arrangement, and degree of matrix cementation. All of these factors also affect the formation permeability. Several studies have confirmed the use of electrical measurements to predict permeability where saline water is present (*e.g.*, Archie, 1950; Jackson *et al*., 1998; Ball *et al*., 1997). Most of the reports concern core-scale relationships, where sample heterogeneity may be less than typically exists at larger scales. Reports of successful use of resistivity measurements to predict permeability at larger scales exist in the case of fresh or nearly-fresh water aquifers (*e.g.*, Croft, 1971; Kwader, 1985).

On this basis, the maximum electrical conductivity ($C_{max} = 1/R_{o,min}$) observed in a well was used to predict that well's flow capacity, measured as the product of permeability and vertical thickness (kh). Core, DST, and production well kh values compared to wireline C_{max} suggest that a useful relationship may exist for the Nisku open marine facies *(Fig. 8)*. Core-based kh values are larger than the DST and production values by about a factor of 20. This is reasonable since locally enhanced permeability will be limited in lateral extent for core, whereas the DST and production values are

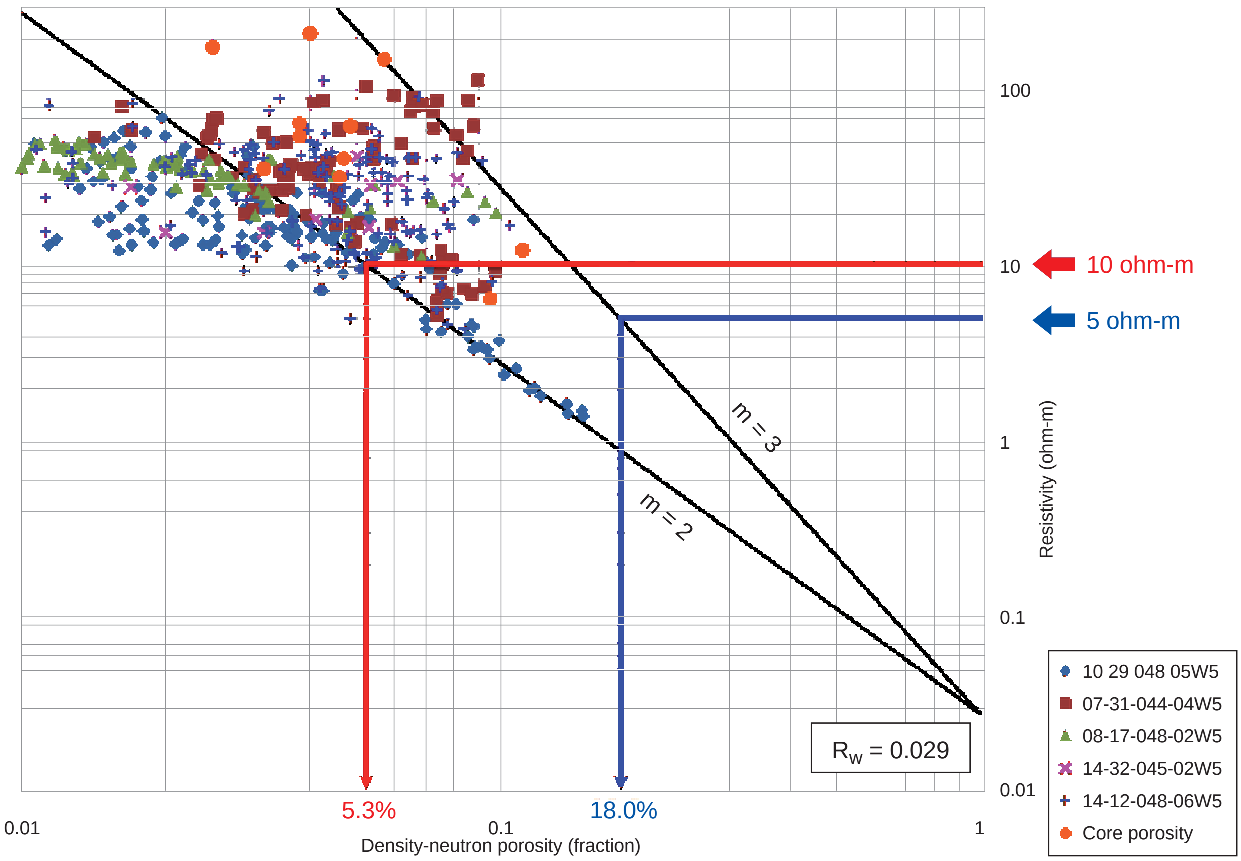

Figure 7

Relationship between deep resistivity wireline data and both core and wireline porosity. Lines are based on Archie's Law. The cementation factor (*m*) value is between 2 and 3 for resistivities below 10 ohm-m. 10 and 5 ohm-m thresholds illustrate range of uncertainty in porosity estimates using this method.

affected by connectivity beyond the near-wellbore region. In addition to the core- and DST-based flow capacities, a *kh* estimate based on reported water well production capabilities of 1000 m^3 per day, is shown in Figure 8. (Assuming a 10 cm radius wellbore and 10% pressure drop to produce a flow of 1000 m^3/day, an estimate of the formation flow capacity is approximately 3000 mD-m.). From the C_{max}—$(kh)_{\text{prod}}$ relationship (lower line of *Fig. 8*), flow capacity values which represent the volumes investigated by DSTs and the production well can be estimated. The C_{max}—$(kh)_{\text{prod}}$ relationship suggests that a minimum electrical conductivity of 150 mhos/m is needed for one Darcy-meter flow capacity to exist. A cumulative distribution function of C_{max} over the AOI (not shown) indicates approximately 25% of wells have $C_{max} > 150$ mmhos/m, suggesting that there are regions with Darcy-meter flow capacity within the Nisku Fm. The location of these wells may prove to be preferable for CO_2 injection.

To test the ability of using C_{max} values to predict flow capacity, we used drilling data. During drilling of nine wells in the WASP area, problems were reported with lost circulation of the drilling mud. For four of these wells, electrical resistivity logs were also available. While there can be a number of reasons why mud losses occur, one such reason is that the well has encountered a large flow capacity interval. The C_{max} values for these four wells exceed 280 mmho/m *(Fig. 9)*, suggesting that electrical conductivity may indeed be responding to the formation flow capacity beyond the wellbore.

4.3 Permeability Estimates

A three-dimensional model of permeability is critical for reservoir characterization and flow simulation. For CO_2 injection, permeability is a very significant variable for controlling total injectivity (*e.g.*, Cinar *et al.*, 2009). Data

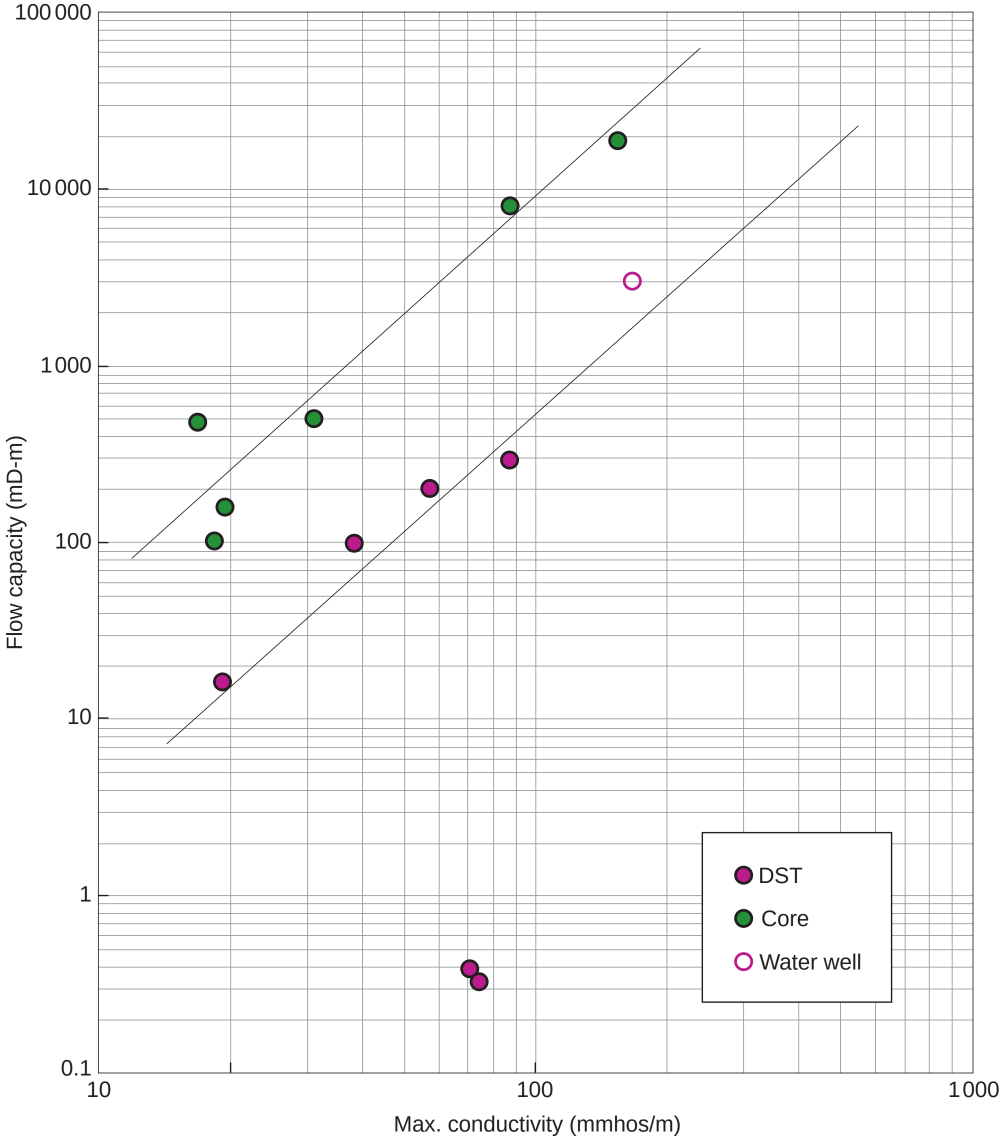

Figure 8

Relationship between maximum conductivity (from wireline logs) and permeability thickness from core (green circles) and DSTs (pink circles). Reasons for the two wells with $(kh)_{DST}$ = 0.3 mD-m to have behaviour different from other wells could not be determined. Open red circle shows water production well (11-29-045-02W5) based on max. conductivity measurement from wireline and estimate of flow capacity based on flow rate.

from cores are a typical source of permeability information, however the Nisku core data suggest much better flow capacities than larger-scale flow tests *(Fig. 8)*. We used the C_{max} *vs kh* relations from core data *(Fig. 8)* to provide an optimistic scenario:

$$kh = 0.33 \cdot C_{max}^{2.2} \quad (3)$$

and a pessimistic scenario, based on DST and production tests:

$$kh = 0.02 \cdot C_{max}^{2.2} \quad (4)$$

C_{max} was evaluated at the same interval as the vertical grid spacing (h) in order to determine an appropriate permeability value to populate the model grid. These values were then used in a conditional simulation to create a three-dimensional model of permeability. Porosity was used as the secondary variable in a colocated co-kriging process. Results for both permeability estimation scenarios were used in the geostatistical modeling, although time constraints limited the flow simulations to be conducted only for the pessimistic case.

Figure 9

Maximum values of wireline conductivity measurements (C_{max}) suggest that wells with no reported kicks or lost circulation (0's) tend to have smaller C_{max} values than those with such events (1's).

4.4 Geomodeling

We applied two modeling approaches for the Nisku aquifer characterization: traditional pixel-based methods and object-based (Boolean) modeling. For the Nisku reservoir model framework, formation tops associated with the Nisku open marine facies were constructed using a convergent interpolation method (Taylor series projection with minimum curvature used for smoothing). As no major faults or other structural displacement features have been identified during the geological analysis, a simple reservoir geometry was sufficient.

From the stratigraphic grid, a cartesian-based model was generated. This model provides the geostatistical framework for subsequent property and petrophysical modeling. The *x* and *y* cell dimensions were fixed at 500 m each direction to satisfy computational constraints of simulating fluid flow for the large region of WASP, while at the same time providing a reasonable level of geological continuity. All data – well paths, well logs, and seismic data were conditioned to the cartesian grid. The vertical layering of the grid was set at 30 layers divided unevenly between the 3 zones *(Tab. 2)* based upon geological interpretations of vertical correlations using the wireline logs. As enhanced porosity and permeability zones appear to exist more frequently in the upper and lower thirds of the reservoir, these vertical intervals benefit from a finer vertical resolution during flow simulation. Wireline logs were upscaled using an arithmetic average for porosity determination and using a harmonic average for vertical permeability (when appropriate). Logs were treated as lines where each sample value is weighted by a factor proportional to its interval.

TABLE 2

Vertical grid spacing for Nisku open marine facies

Vertical layer	Avg thickness (m)	Zone
1-13	1.72	Upper
14-18	4.46	Middle
19-30	1.86	Lower

The variogram analysis established the geological continuity in porosity and permeability for the Nisku reservoir. An assumption is made, however, that the nature of these petrophysical properties is homogeneous at some scale. Both laterally isotropic and anisotropic semivariograms were used, depending on the modeling objective. Spherical variograms were used for lateral correlation, while gaussian variograms were used in the vertical direction. Semivariogram properties were modeled to be anisotropic with a major range of 8 km and minor range of 5 km. Semivariogram ranges on the order of a few kilometers are consistent with depositional patterns found on shallow carbonate platforms (*e.g.* Grant *et al.*, 1994). A trend (N 30 E) was included to reflect alignment of enhanced porosity regions parallel to the paleo-shoreline during upper Devonian deposition. The vertical range was found to be 22 m.

Kriging, as is often observed, produced results that were too smooth to accurately reflect a viable geologic scenario. Therefore, a stochastic (probablistic) method which better recognizes uncertainty and incorporates a factor of randomness (Srivastava, 1994) was applied. Specifically, Sequential Gaussian Simulation (SGS) provided a more

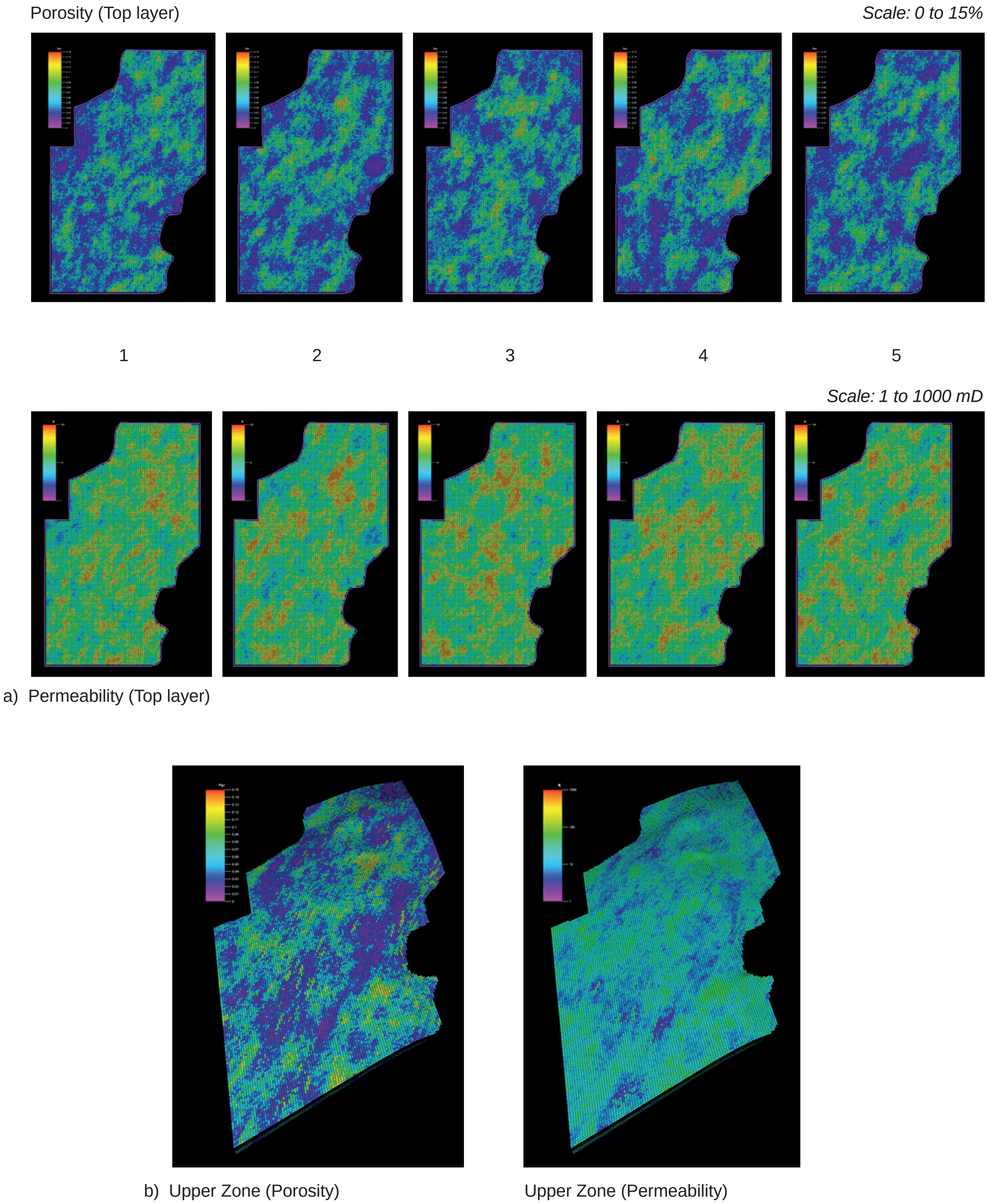

Figure 10

a) Five SGS realizations for Nisku open marine facies porosity (top) and permeability (bottom).

b) Examples of poro-perm distributions based on object-models. Porosity (left) scaled 0 to 15% and permeability (right) scaled 1 to 1000 mD.

realistic distribution of porosities and permeablities *(Fig. 10a)*. As part of this modeling approach, seismic estimates of acoustic impedance were included as a secondary variable for collocated cokriging. (Correlations between seismic attributes and porosity and permeability are widely discussed in the literature. See, for example, Abbaszadeh *et al*. (2004) and Jenkins *et al*. (2008)). Of the fifty realizations generated, five were selected for fluid simulation *(Fig. 10a)*. The realizations developed through SGS methods were qualitatively useful for illustrating potential porosity and permeability distributions in the Nisku open marine facies. Quantitatively, however, the definition of flow pathways over the entire studied region using SGS are poor – again a consequence of limited data. Injectivity volumes (as determined through simulation) provided a useable order-of-magnitude calculation, but there is still a large degree of uncertainty regarding the overall flow connectivity within and between model layers using this method.

Object-modeling (also known as 'Boolean' modeling) provides a method for incorporating plausible and quantifiable three-dimensional facies geometries into the static earth model. This method can provide more plausible geological shapes than cell-based methods, but it is also more difficult to constrain the models to the actual wireline log and/or seismic data sets (Caers, 2005). Already in common use for clastic-systems such as fluvial and submarine channels (*e.g.* Holden *et al*., 1998; North, 1996; Seifert and Jensen, 2000), an object approach to geomodeling may also have application to carbonate systems – especially in cases where larger reservoir areas are being characterized. The dimensions of facies elements (*e.g.* reefs, aprons, and shoals), however, need to be quantified in terms of distribution and geometry – thickness, width, aspect ratio, sinuosity, etc. To our knowledge, studies that include these types of measurements from outcrops or wireline data are very rare (*e.g.* Atchley *et al*., 2002), and thus the application of this method has seen limited use with carbonate systems.

As an alternative source of geometrical data, facies-classified satellite imagery of modern carbonate systems can provide useful quantitative constraints (Harris and Kolwalik, 1994; Andrefouet *et al*., 2001; Andrefouet *et al*., 2003; Bachtel, 2005). For this Nisku study, work by Harris and Vlaswinkel (2008) was especially useful in selecting reasonable parameter values for carbonate-object geometry and scale in the facies being modeled. Dimensions for partially aggraded reef and apron facies (see Harris and Vlaswinkel (2008) for method of facies classification) were chosen as appropriate Nisku open marine facies analogs *(Tab. 3a)*. We assumed that:

- the platform comprises shallow reef systems with an elongated elliptical shape oriented parallel or sub-parallel to the paleo-shore line (approximately N 30 E);
- the reefal buildups were small to intermediate in size (< 200 km^2).

TABLE 3

a) Geometry of enhanced porosity and permeability objects. All distributions are triangular between min., mean, and max.

b) Division of objects based on vertical interval, enhanced regions, and classes. The percent of total volume objects occupy is a controlled parameter subjectively estimated. IBM = inboard margin, OM = open marine

(a)

Enhanced porosity class		Min. (m)	Mean (m)	Max. (m)
Better	Orientation (azimuth)	25	35	45
	Major width	50	500	1200
	Maj./Min. ratio	1	5	7
	Thickness	0.5	5	10
Best	Orientation (azimuth)	25	35	45
	Major width	20	300	800
	Maj./Min. ratio	1	5	7
	Thickness	0.1	2	6

(b)

Vertical zone	Enhanced porosity object fairways	Enhanced porosity class	% of total model volume
Upper	IBM	Better	3%
	IBM	Best	0.5%
	OM	Better	7%
	OM	Best	1%
Middle	IBM	Better	1%
	IBM	Best	0.1%
	OM	Better	4%
	OM	Best	0.5%
Lower	IBM	Better	1%
	IBM	Best	0.1%
	OM	Better	25%
	OM	Best	11%

Vertically, the modeled formation was divided into three roughly proportional zones with distributions of objects variable *(Fig. 11)*. The upper and especially lower zones have the highest propensity for enhanced porosity and permeability objects. Wireline geophysical logs *(Fig. 11)* and the conceptual geology model *(Fig. 3)* provided constraints. Lateral distribution of these objects was subjective, based upon conceptual understandings of the Nisku carbonate platform in the WASP study area *(Fig. 3)*.

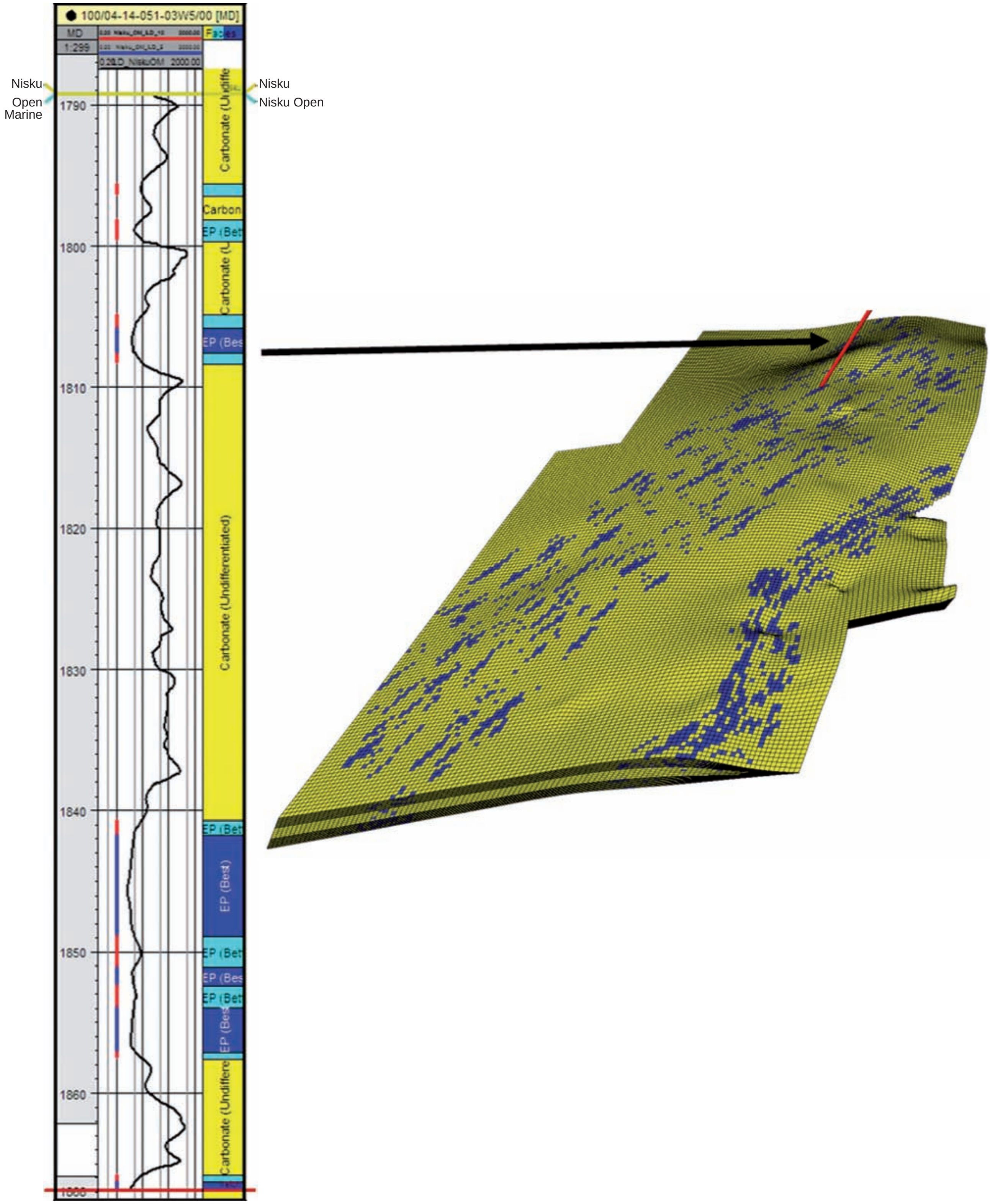

Figure 11

Electrical resistivity (ILD) log for 04-14-051-03W5 (left). Vertical distribution of low resistivity zones used to condition the vertical distribution of enhanced porosity and permeability objects in the model (right). ILD log values below 5 ohm-m are marked by blue and those values below 10 ohm-m are marked by red lines.

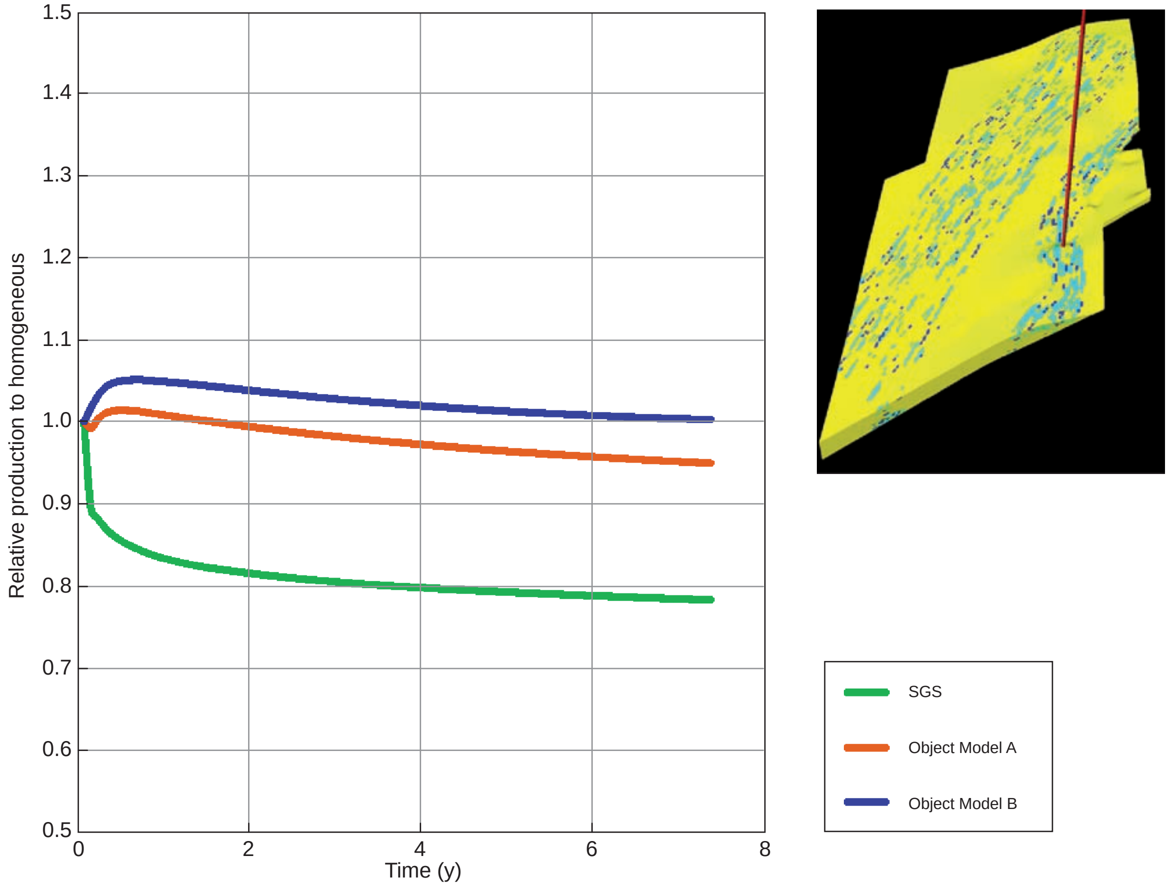

Figure 12

Water production simulation for various model scenarios. Location for water production well (11-29-045-02W5) was used in simulations. SGS – Sequential Gaussian Simulation; Object Model A – one single enhanced poro-perm fairway; Object Model B – two enhanced poro-perm fairways (see inset figure).

Two zones, or fairways, were imposed on the model to reflect a greater likelihood of greater porosity and permeability with better connectivity in these areas. There is some uncertainty, however, as to the existence of better porosity and permeability along the inboard platform margin. The high-capacity water production well suggests the presence of such a zone. Log analysis, however, shows no evidence of improved porosity in the area.

The distribution of objects varied according to the Nisku zone interval being modeled *(Tab. 3)*. All objects were populated stochastically in the system while being conditioned to existing wireline log data. Porosities and permeabilities for objects were determined based on the distribution as determined from wireline conductivity measurements. Two object classes were established:

- better – 8% mean porosity (normal distribution) and 30 mD mean permeability (log-normal distribution);
- best – 14% mean porosity (normal distribution) and 200 mD mean permeability (log-normal distribution);
- SGS was used to populate the non-object filled grid cells.

Several iterations of object distributions were generated and each was then geostatistically populated with flow properties (*Fig. 10b*). The final model was a combination of geologic interpretation and traditional geostatistical methods constrained to available data.

5 MODEL RESULTS

For the Nisku aquifer, the object-based method appears to provide the best order-of-magnitude volume approximations *(Tab. 4)*. The model results suggest pore volumes for the Nisku AOI will be between 15 and 17 km^3, however the real storage potential will be much larger as the aquifer extends far to the northeast and southwest of the study area.

TABLE 4

Minimum potential storage capacity for Nisku reservoir using WASP boundary. Actual volumes will be larger as aquifer extends to the northwest and southeast of study area. Mean permeability (k) is significantly larger for the object model as isolated grid cells containing high values affect the result.

	Bulk volume (10^6 m^3)	Pore volume (10^6 m^3)	Mean ϕ (%)	Mean kh (mD-m)
Homogeneous	305 348	15 267	5.0	2 100
SGS (50 realizations)	305 348	15 258	4.9	70
Object model	305 348	16 924	4.4	46 550

Qualitatively, the potential flow pathways appear most realistic in an object-based model that allows more geologic interpretation of connectivity to be included. The best connected regions are in the lowest third of the Nisku Fm.

While qualitative inspection suggests a more accurate portrayal of mid-to large-scale reservoir heterogeneity using object-based *versus* pixel methods, the models should also be assessed on the basis of their flow performance. Given the limited amount and quality of flow-related data, validation of model behavior is difficult. For example, flow simulations of some DST's could be compared to the field DST's to assess whether permeability and larger-scale connectivity are adequately captured in the models if longer duration and better quality pressure measurements were available. Flow simulations of the water production well, however, are helpful in revealing differences between the models regarding deliverability (up to a maximum of 1000 m^3/day) along the inboard margin region *(Fig. 12)*. All the models tested had sufficient connectivity to deliver water at rates which match actual production for more than 7 years, but the pixel model shows about 25% less connectivity than the object models. This difference could have economically important consequences for development of a sequestration project in the Nisku Fm. Since a development plan will need a model to assess project feasibility and well locations, one or more long-term production tests with proper pressure and flow monitoring are needed to help decide which model is more appropriate.

Other studies have investigated geomechanical (Goodarzi *et al*., 2010), geochemical (Hutcheon, 1999), and fluid flow aspects of the Nisku Fm. Fluid flow simulations of CO_2 injection were made using the heterogeneous models produced for this project (see Ghaderi *et al*., 2008). Results indicate total capacity will be below the original target volume of 20 Mt/yr *(Fig. 13)*. From the available data, higher permeabilities (> 100 mD) are not modeled to have the connectivity necessary to accommodate such large injection volumes. The locations of injection wells in the flow simulations can affect injectivity, by only the order of +/– 5% at most. Horizontal drilling and hydro-fracturing, however, may double the total injection capacity (Ghaderi *et al*., 2009).

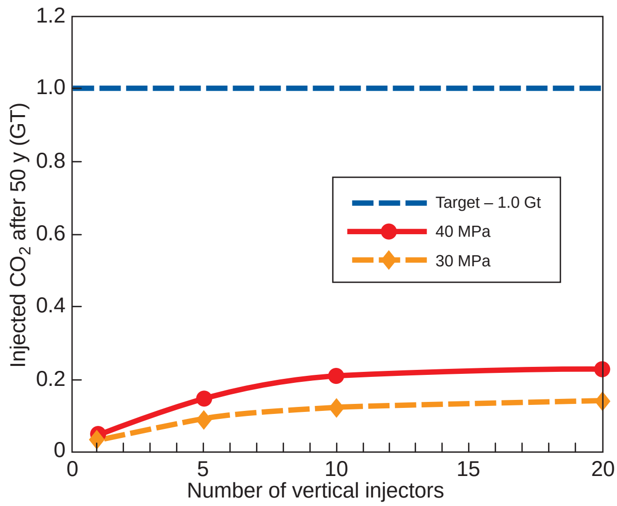

Figure 13

For homogeneous reservoir case (k = 30 mD, ϕ = 8%) showing injection potential as a function of reservoir fracture pressure. A minimum of 10 injectors is necessary to achieve 0.2 Gt after 50 years. Only a slight increase is obtained using 20 injectors.

CONCLUSIONS

The available core analyses and petrophysical evaluation of wireline logs indicate average porosities for the Nisku interval to between 3 and 5%, with localized zones in excess of 10%. Permeability from core measurements shows the median to be 10 mD, but with some values in excess of several Darcys. In trying to map the distribution, size, and connectivity of these better porosity-permeability intervals, wireline logs were used.

Wireline log resistivity measurements provided a useful tool to estimate both the minimum porosity and permeability. Log and core data indicate that the Archie cementation factor m is between 2 and 3. This variability causes resistivity-based porosity estimates to be quite variable, but assuming m = 2 provides a useful estimator of minimum porosity. Using this method, zones with porosity greater than 8% were more often in the lower third of the reservoir interval. Formation flow capacities, estimated using a relationship between maximum wireline conductivity and permeability thickness from core and DST data, were up to several Darcy-meters in the best cases. The flow capacity is greater than 1 D-m for 25% of the wells using the conductivity—flow capacity relationship. Wells with mud losses during drilling correlated with wells having larger electrical conductivities, supporting the existence of a relationship between the electrical and hydraulic characteristics.

For characterization of the Nisku Fm. in the Wabamun study, object methods may have advantages for integration of conceptual geologic information over traditional pixel-based methods using semivariograms. Variogram based methods struggle to accurately model reservoirs where depositional bodies and geologic shapes (which are typically curvilinear) control the distribution of flow properties (*i.e.* porosity and permeability). For carbonate systems, the application of object-based models has seen limited application, primarily due to the problem of defining carbonate depositional geometries and distributions and the impression that random, diagenetic influences are more important than depositional characteristics. Some of these challenges were addressed in this study using satellite-based facies mapping of modern analogues and inferences based on existing knowledge of the Nisku Fm. While many limitations remain, object -based geomodeling for large regional-scale carbonates with sparse data shows promise.

The static-earth models were exported for use in fluid-flow simulations. The petrophysical analysis and geomodeling suggests potentially good injection volume and flow capacity in the Nisku assuming the best interval and laterally extensive zones are targeted. Seismic data will be invaluable in this process. Another concern is the fracture pressure of the reservoir, which requires detailed geomechanical understanding and a well integrated model of the caprock – in this case the formations of the Winterburn aquitard. The geological model created here can be used as part of this process. Finally, it is necessary to validate the static models for accuracy. This can be done using simulated DSTs and by regenerating models when new data become available. Simulations of the one water production well along the inboard margin suggest there can be important differences in connectivity between models.

Reservoir rock properties and configuration suggest the Nisku formation may be a potentially valuable CO_2 injection and storage target for the Wabamun region. As previous investigators concluded (Michael *et al*., 2009), the Devonian strata provide a suitable candidate for sequestration presently. The regional characterizations, however, also suggests the need for more detailed site-specific information, especially seismic data acquisition, in order to assess potential injection targets properly.

ACKNOWLEDGMENTS

We thank the numerous sponsors of the WASP project for financial support, which include Alberta Energy Research Institute (AERI), Natural Sciences and Engineering Research Council (NSERC), TransAlta, TransCanada, ARC Energy Trust, Penn West Energy Trust, Epcor, Enbridge, ConocoPhillips Canada, Encana, StatOilHydro Canada, Total Canada, Computer Modeling Group, and Golder Associates. The editorial and review comments greatly improved this manuscript. Jerry L. Jensen holds the Schulich Chair in Geostatistics at the University of Calgary.

REFERENCES

Abbaszadeh M., Takahashi I., Suzuki K. (2004) Integrated Seismic-Guided Characterization of a Carbonate Reservoir in Abu Dahbi, U.A.E., SPE 90533 presented at the *SPE Annual Technical Conference and Exhibition in Houston*, TX, Sept. 26-29.

Alshuhail A., Lawton D., Isaac H. (2009) Acoustic Impedance Inversion of Vintage Seismic Data Over a Proposed CO_2 Sequestration Site in the Lake Wabamun Area, Alberta, *CREWES Research Report* **20**, 1-20.

Andrefouet S., Claereboudt M., Matsakis P., Pages J., Dufour P. (2001) Typology of Atoll Rims in Tuamotu Archipelago (French Polynesia) at Landscape Scale Using SPOT HRV Images, *Int. J. Remote Sens.* **22**, 6, 987-1004.

Andrefouet S., Kramer P., Torres-Pulliza D., Joyce K.E., Hochberg E.J., Garza-Perez R., Mumby P.J., Riegl B., Yamano H., White W.H., Zubia M., Brock J.C., Phinn S.R., Naseer A., Hatcher B.G., Muller-Karger F.E. (2003) Multi-site Evaluation of IKONOS Data for Classification of Tropical Coral Reef Environments, *Remote Sens. Environ.* **88**, 1-2, 128-143.

Archie G.E. (1942) The Electrical Resistivity Log as an Aid in Determining Some Reservoir Characteristics, *Am. Inst. Min. Met. Eng. T.* **146**, 54-62.

Archie G.E. (1950) Introduction to Petrophysics of Reservoir Rocks, *B. Am. Ass. Petrol. Geol.* **34**, 943-961.

Atchley S., McMurray M. (2002) Devonian (Frasnian) Leduc- and Nisku-equivalent Outcrops Near Canmore, Alberta: 1-D Outcrops as a Guide to Subsurface Stratal Architecture, *Am. Ass. Petrol. Geol. Annual Conv.*, Houston, Texas.

Attia A.M., Fratta D., Bassiouni Z. (2008) Irreducible Water Saturation from Capillary Pressure and Electrical Resistivity Measurements, *Oil Gas Sci. Technol.* **63**, 2, 203-217.

Bachtel S.L. (2005) Platform-scale Facies Distributions Using Landsat Data from Isolated Carbonate Platforms: Methods to Constrain Lateral Facies Continuity for Geologic Modeling, *Am. Ass. Petrol. Geol. Annual Conv.,* Calgary, Alberta.

Bachu S., Bennion B. (2008) Effects of *In-situ* Conditions on Relative Permeability Characteristics of CO_2-brine Systems, *Environ. Geol.* **54**, 8, 1707-1722.

Ball L.D., Corbett P.W.M., Jensen J.L., Lewis J.J.M. (1997) The Role of Geology in the Behavior and Choice of Permeability Predictors, *SPE Formation Evaluation* **12**, 1, 32-39.

Caers J. (2005) *Petroleum Geostatistics*, Soc. for Petro. Eng., Richardson, Texas.

Cinar Y., Neal P.R., Allinson W.G., Sayers J. (2009) Geo-engineering and Economic Assessment of a Potential Carbon Capture and Storage Site in Southeast Queensland, Australia, *SPE Reserv. Eval. Eng.* **12**, 5, 660-670.

Croft M.G. (1971) A Method of Calculating Permeability from Electric Logs, *U. S. Geol. Survey. Prof. Paper* ***750-B***, 265-269.

Environment Canada (2009) *National Inventory Report 1990-2007: Greenhouse Gas Sources and Sinks in Canada*, Greenhouse Gas Division, Gatineau. http://www.ec.gc.ca/pdb/ghg/inventory_report/2007/som-sum_eng.pdf.

Ghaderi S.M., Keith D.W., Leonenko Y. (2009) Feasibility of Injecting Large Volumes of CO_2 in Aquifers, *9th International Conference on Greenhouse Gas Control Technologies (GHGT-9)*, Washington DC, November 16-20.

Goodarzi S., Settari A., Keith D.W. (2010) Geomechanical Modeling for CO_2 Storage in Wabamun Lake Area of Alberta, Canada, *10th International Conference on Greenhouse Gas Control Technologies (GHGT-10)*, Amsterdam, September 19-23.

Grant C.W., Goggin D.J., Harris P.M. (1994) Outcrop Analog for Cyclic-Shelf Reservoirs, San Andreas Formation of Permian Basin: Stratigraphic Framework, Permeability Distribution, Geostatistics, and Fluid-Flow Modeling, *B. Am. Ass. Petrol. Geol.* **78**, 23-54.

Harris P.M., Kolwalik W.S. (1994) Satellite Images of Carbonate Depositional Settings: Examples of Reservoir- and Exploration-scale Geologic Facies Variation, *Am. Ass. Petrol. Geol., Methods in Exploration Series* **11**, 1-147.

Harris P.M., Vlaswinkel B. (2008) Modern Isolated Carbonate Platforms: Templates for Quantifying Facies Attributes of Hydrocarbon Reservoirs, *Soc. Sed. Geol. Special Pub.* **89**, 323-341.

Hitchon B. (1996) *Aquifer Disposal of Carbon Dioxide*, Geoscience Publishing Ltd., Sherwood Park, Alberta.

Holden L., Hauge R., Skare O., Skorstad A. (1998) Modeling Fluid Reservoirs with Object Models, *Math. Geol.* **30**, 5, 473-496.

Hutcheon I. (1999) Controls on the Distribution of Non-Hydrocarbon Gases in the Alberta Basin, *B. Can. Ass. Petrol. Geol.* **47**, 573-593.

Jackson P.D., Harvey P.K., Lovell M.A., Gunn D.A., Williams C.G., Flint R.C. (1998) Measurement Scale and Formation Heterogeneity: Effects on the Integration of Resistivity Data, *Geol. Soc. Special Publication* **136**, 261-272.

Jenkins C.C., Chiquito P.N., Mills A.A., McPherson J.G., Schapper M.C., Williams M.A. (2008) Reservoir Definition at the Jansz/Io Gas Field, NW Shelf, Australia: A Case Study of an Integrated Project From Exploration to Development, IPTC 12461 presented at the *Int. Petroleum Tech. Conference,* Kuala Lumpur, Malaysia, Dec. 3-5.

Kwader T. (1985) Estimating Aquifer Permeability from Formation Resistivity Factors, *Ground Water* **23**, 6, 762-766.

Lucia J.F. (2007) *Carbonate Reservoir Characterization: An Integrated Approach*, Springer, Berlin.

Machel H.G. (1985) Facies and Diagenesis of the Upper Devonian Nisku Formation in the Subsurface of Central Alberta, *PhD Thesis*, McGill University.

Michael K., Bachu S., Buschkuehle B.E., Haug K., Grobe M., Lytviak A.T. (2006) Comprehensive Characterization of a Potential Site for CO_2 Geological Storage in Central Alberta, Canada, *CO2SC Symposium*, Berkeley, California.

Michael K., Bachu S., Buschkuehle B.E., Haug K., Talman S. (2009) Comprehensive Characterization of a Potential Site for CO_2 Geological Storage in Central Alberta, Canada in *Carbon Dioxide Sequestration in Geological Media – State of the Art*, Grobe M., Pashin J., Dodge R. (eds), AAPG Studies in Geology **59**, Tulsa, Oklahoma.

Mossop G.D., Shetsen I. (comps.) (1994) *Geological Atlas of the Western Canada Sedimentary Basin*, Canadian Society of Petroleum Geologists and Alberta Research Council, Special Report 4, Calgary, Alberta.

North C.P. (1996) The Prediction and Modeling of Subsurface Fluvial Stratigraphy in *Advances in Fluvial Dynamics and Stratigraphy*, Carling P.A., Dawson M.R. (eds), John Wiley and Sons, New York.

SCG Ltd., Stoakes Consulting Group (2009) Personal communication.

Seifert D., Jensen J.L. (2000) Object and Pixel-based Reservoir Modeling of a Braided Fluvial Reservoir, *Math. Geol.* **32**, 5, 581-603.

Simpson G.P. (1999) Sulfate Reduction and Fluid Chemistry of the Devonian Leduc and Nisku Formations in South-central Alberta, *PhD Thesis*, University of Calgary.

Srivastava R.M. (1994) An Overview of Stochastic Methods for Reservoir Characterization in *AAPG Computer Applications in Geology No. 3, Stochastic Modeling and Geostatistics: Principles, Methods and Case Studies*, Yarus J.M., Chambers R.L. (eds), American Association of Petroleum Geologists, Tulsa, Oklahoma.

Stoakes F.A. (1987) Evolution of the Upper Devonian of Western Canada in *Principles and Concepts for Exploration and Exploitation of Reefs in the Western Canada Basin: Short Course Notes, Canadian Reef Inventory Project*, Canadian Society of Petroleum Geologists, Calgary, Alberta.

Stoakes F.A. (1992) Winterburn Megasequence in *Devonian - Early Mississippian Carbonates of the Western Canada Sedimentary Basin: A Sequence Stratigraphic Framework*, Wendte J.C., Stoakes F.A., Campbell C.V. (eds), Society of Economic Paleontologists and Mineralogists Short Course No. 28, Calgary, Alberta.

Switzer S.B., Holland W.G., Christie D.S., Graf G.C., Hedinger A.S., McAuley R.J., Wierzbicki R.A., Packard J.J. (1994) Devonian Woodbend - Winterburn Strata of the Western Canada Sedimentary Basin in *Geological Atlas of the Western Canada Sedimentary Basin*, Mossop G.D., Shetsen I. (comps.), Canadian Society of Petroleum Geologists and Alberta Research Council, Special Report 4, Calgary, Alberta.

Watts N.R. (1987) Carbonate Sedimentology and Depositional History of the Nisku Formation in South-central Alberta in *Devonian Lithofacies and Reservoir Styles in Alberta*, Krause F.F., Burrows O.G. (eds), *2nd International Symposium of the Devonian System*, *13th CSPG Core Conference*, Calgary, Alberta.

Wylie M.R., Gregory A.R., Gardner L.W. (1956) Elastic Wave Velocities in Heterogeneous and Porous Media, *Geophysics* **21**, 41-70.

Final manuscript received in July 2009
Published online in February 2011